CARDIAC OUTPUT VARIABILITY DURING INDUCTION OF HYPOVOLEMIC SHOCK

Joyce da Silva Bevilacqua[1,2]
[1] Centro Universitário Senac – Campus Santo Amaro. Av. Eng. Eusébio Stevaux, 823, 04696-000, São Paulo, SP, Brasil.
joyce.bevilacqua@sp.senac.br
[2] Instituto de Matemática e Estatística da Universidade de São Paulo.
Rua do Matão, 1010, 05508-900, São Paulo, SP, Brasil.
joyce@ime.usp.br
Gislaine Silva Vieira Duarte
Instituto de Matemática e Estatística da Universidade de São Paulo.
Rua do Matão, 1010, 05508-900, São Paulo, SP, Brasil.
gislaine@ime.usp.br

Abstract. *Hypovolemic shock was induced in fourteen male rats by successive bleeding. During 30 minutes, after base signal acquisition, 3.1ml of blood for each 100g of weight has been collected. After this period,a treatment was initiated with isotonic saline solution (7.5%NaCl each 0.4ml/g of weight) or hypertonic (0.9% NaCl each 0.4ml/g of weight). The arterial pressure signal was captured during all the experiment. The goal of this work is to analise the variability of the cardiac debit during the induction of shock and identify whether the physiologic mechanism to compensate the loss of volume is working. The analysis is foccused on the cardiac debit, because it depends linearly on systolic volume and heart rate. A non-invasive method was implemented to calculate the systolic volume directly from the arterial pressure signal. Wavelet analysis was used to find the main frequencies and also their variability during each stage. The cardiac debit stability was expected, because the heart rate must increase to compensate the lost of volume. In both cases was observed that the frequency increase in the stage E1 followed by a significant decrease. As a consequence the cardiac debit descreases during the intermediat stages, showing that the compensation mechanism was not working propely. In three experiments the frequencies increase only in the final stage. This anomalie suggests a deeper investigation including response to treatment and shock evolution.*

Keywords*: signal processing, wavelet, variability, cardiac debit, shock.*

1. INTRODUCTION: INDUCTION OF CIRCULATORY SHOCK

Circulatory system is responsible to maintain the blood circulating through the body providing oxygen to cells and its efficiency can be monitored by the cardiac output. During physical exercises or stress situations a compensation mechanism is immediately activate, inducing changes in arterial pressure and heart rate to maintain the systolic volume adequate to perfusion (Guyton, 2002). Hemodynamic and metabolic disturbance occurs in the absence of this mechanism. Shock is caused by hemorrhagy, heart infection, heart failure, septicemia or infectious agents present in the blood, but in all cases occurs a significant reduction of blood flow which induces blood pressure to decrease critically in order to preserve vital organs. Depending on its severity a progressive processes could be installed and, as a consequence of a not sufficient delivery of oxygen, the damage to tissues and vital organs could be permanent or causes the death of the patient (Rocha and Silva, 1973). Understand failures of compensation mechanism, identify favorable conditions to complete recover is still an important subject.

During the induction of hypovolemic shock, chemoreceptors reflexes, baroreceptors reflexes and ischemia, stimulate a physiological response which changes the arterial pressure and heart rate. An intense vasoconstriction and increased heart rate try to maintain the oxygen delivery. In progressive shock the mechanism alone is not able to compensate the loss of volume, increasing the severity of the shock if no treatment is initiates. Unfortunately, even under critical care treatment, a positive evolution is not guaranteed.

Hypovolemic shock was induced in fourteen male rats Wistar by eight successive bleeding. The experiment was coordinated by Dr. Francisco Soriano, in the Laboratory of Medical Investigation of Medical School of University of São Paulo. Each rat was identified by $\boldsymbol{Rk}$, $\boldsymbol{k}$ = 1, 2,..., 14 and weighted. The weights vary from 250g to 380g. The same protocol was applied to all animals: a catheter was inserted in the femoral artery and a base signal of arterial pressure captured; a sequence of eight bleeding episodes, in each one 3.1ml of blood for each 100g of rat weight was extracted; a final episode, the rat was observed during 30 minutes and after this period an injection of isotonic saline solution (7.5%NaCl each 0.4ml/g of weight) or hypertonic (0.9% NaCl each 0.4ml/g of weight) was administrated. The arterial pressure signal was captured during all the experiment, in a rate of 200 samples per second by Biopac System Inc. apparatus. Data noise and inconsistency were removed by Biopac before save in txt format.

The graphic in Fig. 1 shows the complete data acquisition for the rat ***R6***. A hypothesis that must be investigated is the correlation between the variability of arterial pressure, heart rate and final outcome in the shock. Recent studies propose the heart rate variability as an index of the autonomic regulation of circulatory function: great variability increases the chance of circulatory system recovery. As a controversy topic the discussion is not ended (Parati *et al*, 1991). However, as the signal of arterial pressure is very sensitive to small perturbations in blood volume and heart

frequency our study is a first step in the direction to identify the possibility to detect this variability. Wavelet analysis is used for this purpose (Cerutti *et al.*, 1991).

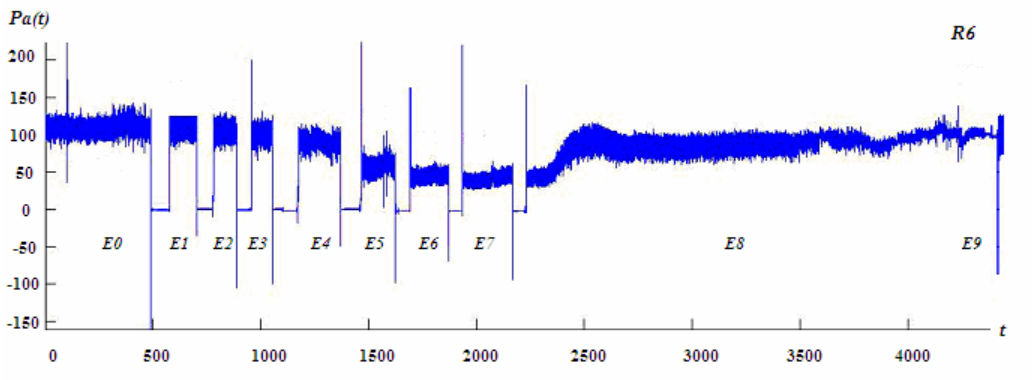

Figure 1. Arterial pressure signal during experiment of induction of hypovolemic shock.

The goal of the compensation mechanism is to maintain perfusion and consequently oxygen delivery. During the successive bleeding episodes is expected an increase of the heart rate followed by decreasing of arterial pressure. During the final episode, in the first 30 minutes a stabilization of perfusion is also expected, demonstrating the system capability to transpose interstitial water to main circulation. After treatment the volume returns to normal levels and another stabilization of frequency and pressure is expected.

The analysis in this work is over the arterial pressure signal. A first algorithm identify the ten intervals of ***Ik***, ***k = 0, 1, …, 9,*** each one corresponding respectively to the ***Ek*** episode. This algorithm also excludes samples collected at the beginning and at the end of each episode which do not fit physiological values. Extraction of blood and manipulation of the animal causes great variation in the signal in the interval extremes of each episode, these data are not excluded by Biopac because their magnitude is not compatible to error acquisition.

After identification of each episode, in section 2 the systolic volume and heart rate are calculated in function of pressure signal. Local values can be calculated but the analysis was done comparing the mean values of systolic volume and heart rate. The frequency is calculated by two different methods in section 3. The classic method counts the number of entire cardiac cycle per minute and the other method uses wavelet analysis of arterial pressure signal, defining the heart rate as the maximal frequency of the signal. Section 4 shows the results and final conclusions in terms of the cardiac output, defined as the systolic volume ejected by heart per minute.

2. ARTERIAL PRESSURE SIGNAL AND SYSTOLIC VOLUME

The first mathematical equation describing cardiac output (D_c) was published by Adolph Fick, in 1870 (Gottschall, 1999, and Introcaso, 1998):

$$D_c(ml/min) = \frac{VO_2(ml/min)}{CaO_2 - CvO_2(ml/100ml)}, \tag{1}$$

VO_2 is the oxygen consumption per minute and CaO_2 - CvO_2 is the difference between the volume of oxygen present in arterial and venous circulation, respectively, each 100 ml of blood. This formula allows to evaluate the cardiac pump and to calculate an approximation of the systolic volume, by dividing the cardiac output by the heart rate, as shows Eq. (2):

$$D_c = V_s.F_c, \tag{2}$$

V_s is the systolic volume, the volume of blood delivered by heart per minute and F_c is heart rate, the number of heart beats per minute. Mathematically, the flow through a duct depends linearly on the difference of pressure (ΔP) and on the inverse of duct resistance (R). So the cardiac output can be expressed by:

$$D_c = \frac{\Delta P_a}{R}. \tag{3}$$

The index a in P_a represents the arterial pressure. From Eq. (2) and Eq. (3) the dependence between these four parameter, D_c, V_s, F_c, P_a is immediate and induce the use of the most suitable method of data acquisition.

$$\Delta P_a = R.V_s.F_c, \tag{4}$$

The algorithms implemented in this work are based on these theoretic arguments, and use only the temporal series of arterial pressure $P_a(t)$, as input data to estimate V_s and F_c.

Considering a period of time greater than one heart beat, four critical points could be identified in the $P_a(t)$ curve. Point **A** identify the beginning of the cardiac cycle; point **B** the beginning of the relaxation of the left ventricle followed by a very slow decrease of $P_a(t)$; point **C** identify the end of the pressure decrease; point **D** the closure of the aorta valve and consequently the end of systolic period. Figure 2 shows the values of $P_a(t)$ during four complete cycles and the locations of the points **A**, **B**, **C** and **D**.

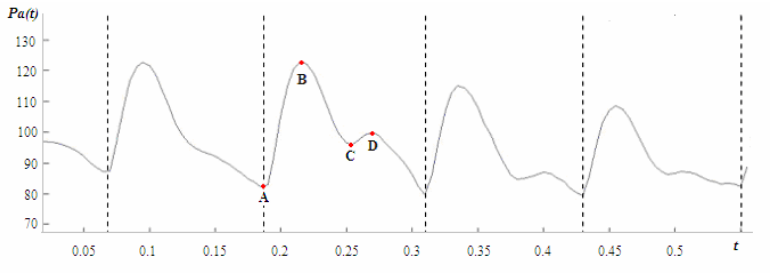

Figure 2. Critical points during cardiac cycle in the signal of arterial pressure $P_a(t)$.

If the signal of $P_a(t)$ is captured in a peripheral arterial vase or in abnormal cardiovascular situations, the points **C** and **D** can not be detected, as is shown in Fig. 3. Detection of critical points is done based on the discrete differential of $P_a(t)$, where the variations due to error signal acquisition are eliminated. The detection algorithm was validated initially considering well known periodic functions and when applied to a general signal the result is visualized matching the original curve and the detected points.

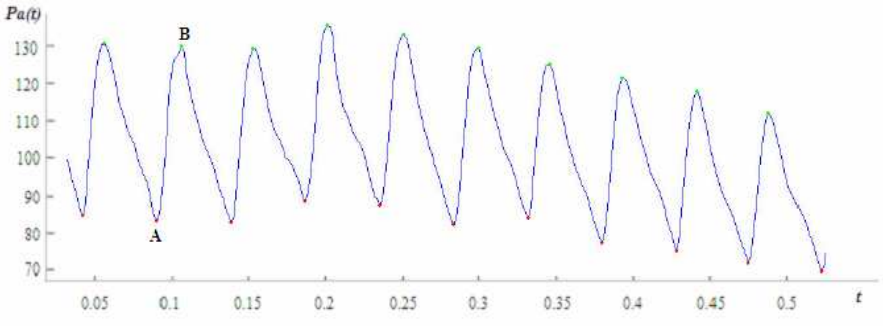

Figure 3. Visualization of the detection algorithm to find points **A** and **B** in the signal of $P_a(t)$.

2.1. Systolic volume

Cerutti *et al.* (2001), showed that the systolic volume is highly correlated to the integrals:

$$\int_A^B P_a(t)dt\,, \qquad \int_A^C P_a(t)dt\,. \tag{5}$$

In this work Cerutti *et al*. proved that the correlations between these integrals and measured systolic volume are very high, precisely equal to $r = 0.96$ for the first integral and $r = 0.97$ for the second. This guarantees that both integrals can be used to estimate V_s. However, the end of the ejection phase, or the point **C,** is not always detectable, therefore the first integral is more efficient, for the systolic peak, or the point **B**, is always detectable.

The algorithm to calculate V_s from the signal of $P_a(t)$ was implemented, assuming that the normalization constant defines the approximated values of V_s as a pure number by:

$$V_s = \int_A^B P_a(t)dt\,. \tag{6}$$

Mean value of V_s was calculated for each episode and each animal. Table 1 shows the mean and standard deviation values for each episode, considering all the individual results. Expected results for normal function of circulatory system were observed: the systolic volume decreases until the episode ***E8*** and recovers the volume in the last one. An isolated recovery during the experiment, as observed in episode ***E4***, is common in the first 5 episodes. It means that the

body succeeded to compensate the loss of volume by increasing frequency in that episode. However, the compensation mechanism can not be sustained and a volume decrease is observed already in the next episode. Individual results are not so consistent with the expected result because during some experiments great variations of the $P_a(t)$ signal were observed, indicating abnormality in the compensation mechanism as occurred with rat ***R1***, showed in Tab. 2 and Fig. 4.

As the experience focused on the capture of pressure curves during induction of hypovolemic shock, data is not collected after episode ***E9***. Abnormality, even when identified, can not be diagnosed. During the experiment the position of the catheter is maintained, suggesting that the abnormality observed in rat *R1* is caused by cardiac frequency oscillation instead of variation in the peripheral resistance. The ideal balance of Eq. (4) is obtained by a positive variation of the cardiac frequency proportional to the inverse of volume variation. The episodes ***E3***, ***E4***, ***E5*** and ***E6***, of Tab. (2), show a tendency to recover to a normal level for $P_a(t)$, but the instability of episodes ***E1***, ***E2***, ***E7***, ***E8*** and ***E9*** demonstrated that the compensation is not consistent.

Table 1. Mean and standard deviation values of systolic volume calculated for each episode.

V_s	*E0*	*E1*	*E2*	*E3*	*E4*	*E5*	*E6*	*E7*	*E8*	*E9*
M	0.54	0.54	0.48	0.47	0.50	0.46	0.43	0.41	0.35	0.71
DP	0.15	0.14	0.13	0.12	0.14	0.15	0.13	0.14	0.09	0.32

Table 2. Mean values of systolic volume calculated for each episode for rat *R1*.

V_s	*E0*	*E1*	*E2*	*E3*	*E4*	*E5*	*E6*	*E7*	*E8*	*E9*
R1	0.25	0.35	0.24	0.21	0.18	0.20	0.34	0.62	0.37	1.14

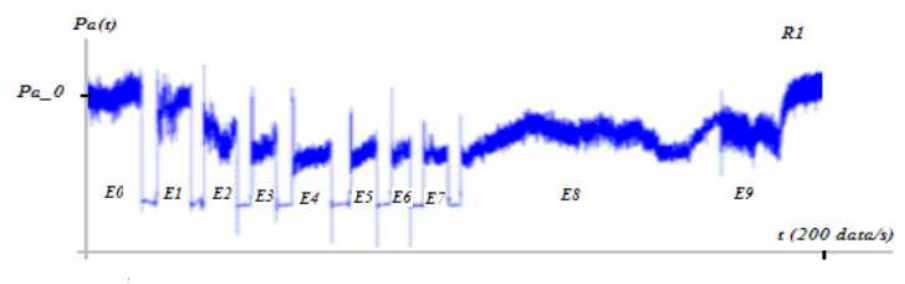

Figure 4. Experimental arterial pressure data for rat *R1*.

3. ARTERIAL PRESSURE SIGNAL AND HEART RATE

The heart rate is calculated by two different methods. Method **M1** is the canonic calculation, which estimates the period π_c of one cardiac cycle by the distance between two consecutives points **A** (Godje *et al*, 2001). F_c is given by

$$F_c = \frac{60}{\pi_c} \tag{7}$$

Method **M2**, estimates de frequency by the wavelet approximation of $P_a(t)$ signal (Cerutti *et al*. 2001). The hypothesis is that this method could detect subtle variations of frequency non detectable by method M1.

Arterial pressure curve is a periodic non-stationary signal with means that its inherent characteristics vary in time. Classical Fourier analysis applied to this signal is able to identify the main frequencies but can not identify when they occur. Short-time Fourier transform, introduces the concept of windowing, which uses a smooth function, defined in an interval (window) for segmentation and the complete time-frequency distribution can be recovered. However, the disadvantage of this technique is related to the window length that must be fixed in advance. Short and long windows could not detect, respectively, low frequencies and short pulses, compromising the resolution. Wavelet transform transpose this limitation introducing the concept of variable window.

The wavelet transform of a discrete signal (t_k, $f(t_k)$), k = 1, 2,..., N, is defined by

$$TW(a,b) = \sum_{k=0}^{N-1} f(t_k)\psi_{a,b}(t_k) = \left\langle f(t), \overline{\psi}_{a,b}(t) \right\rangle \tag{8}$$

where, the function $\Psi_{a,b}(t)$, given by Eq. (9), is a basis function generated by the mother-wavelet. The parameter $a > 0$ defines the scale and b the shift.

$$\psi_{a,b}(t_k) = \frac{1}{\sqrt{a}}\psi\left(\frac{t_k - b}{a}\right) \tag{9}$$

In this study, the mother-wavelet was defined in terms of the spectrum dispersion index calculated for the basal signal. This index measures the spectral occupation and energy concentration of the signal in a fixed interval. Frequency is better defined for great values of this index. The index was calculates for different types of mother-wavelet, different values of maximal frequency (F_{max}) and total number of samples **N**. Table 3 shows the result for fixed values of F_{max} and N. Figure 5 shows the difference between two mother-wavelet in the spectral map, for F_{max} = 50 and N = 64, demonstrating that for the Haar basis the main frequency is not well defined and Fig. 6 shows the spectral map for different values of N. Morlet-basis is used to detect the main frequency in all episodes and N = 64, for the same reason. In all cases the scale is defined by

$$a_j = \frac{F_{max}}{j}, \; j = 1, 2, ..., \text{N} \tag{10}$$

Table 3. Spectrum dispersion index with F_{max} = 50.

Mother-wavelet	N = 32	N = 64	N = 128	N = 256
Db2	3.1172	3.2074	3.1879	3.1261
Dmey	5.0523	5.777	5.6435	5.4731
Haar	1.6509	1.6253	1.5995	0
Mex. hat	2.7428	2.7681	2.6652	2.6090
Morlet	9.5905	9.8223	8.6930	8.2741

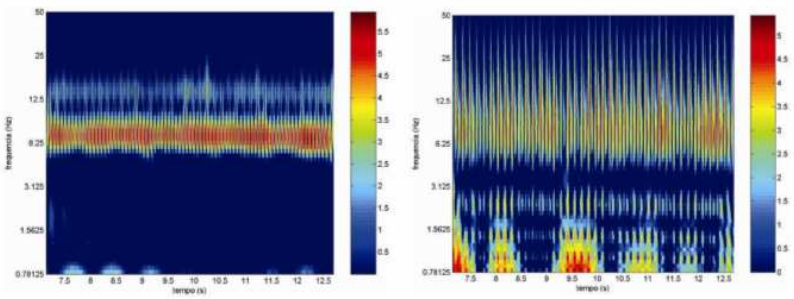

Figure 5. Spectral map for Morlet-wavelet (left) and Haar-wavelet (right).

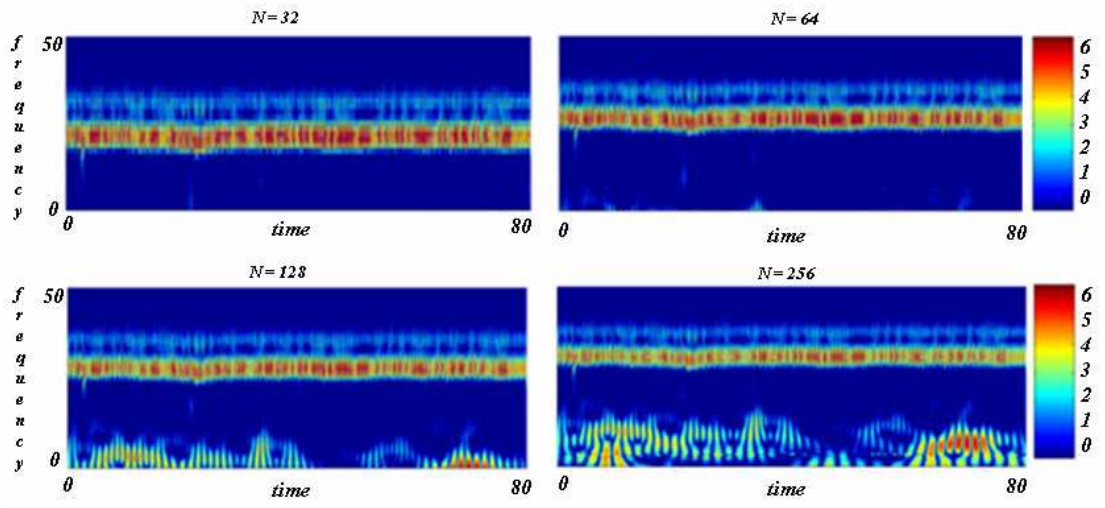

Figure 6. Spectral map for Morlet-wavelet and different values of N.

4. ANALYSIS OF THE CARDIAC OUTPUT

Cardiac output is defined by Eq. (11) and in this work we use two different methods to calculate the heart rate. Table 4 and Fig. 7, show the mean values of cardiac output for the method M1. Table 5 and Fig. 8 show the mean values of cardiac output for the method M2.

$$D_c = V_s.F_c \tag{11}$$

Table 4. Mean cardiac output calculating F_c by method M1.

DC_1	*E0*	*E1*	*E2*	*E3*	*E4*	*E5*	*E6*	*E7*	*E8*	*E9*
M	0,44	0,46	0,44	0,40	0,74	0,65	0,62	0,66	0,73	0,86
DP	0,12	0,12	0,10	0,09	0,09	0,10	0,13	0,12	0,12	0,08

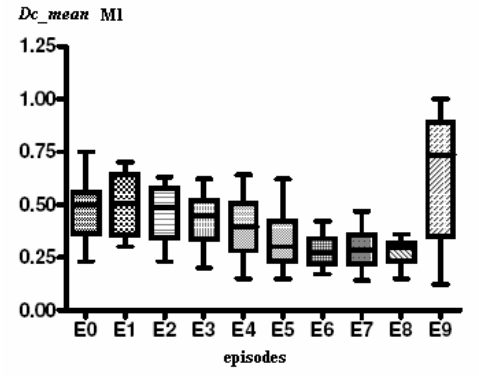

Figure 7. Mean cardiac debt using method M1.

Table 5. Mean cardiac output calculating F_c by method M2.

DC_1	*E0*	*E1*	*E2*	*E3*	*E4*	*E5*	*E6*	*E7*	*E8*	*E9*
M	0,49	0,50	0,47	0,43	0,39	0,32	0,28	0,29	0,28	0,64
DP	0,15	0,14	0,12	0,12	0,14	0,12	0,07	0,09	0,06	0,28

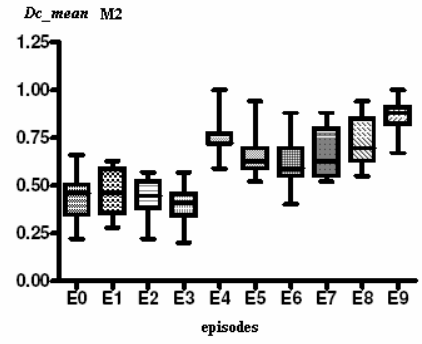

Figure 8. Mean cardiac output using method M2.

In both cases the mean cardiac output increases in the episode E1 and decreases in E2 and E3 as was expected, demonstrating consistency of M2. After episode E3, the two methods showed very different behavior. For M2, a kind of discontinuity is observed between E3 and E4 and the frequency is higher than the ones calculated by M1. The compensation mechanism seems to work better for M2 evaluations because the evolution indicates the tentative to maintain cardiac output, even with successive bleeding. However, to confirm this thesis, the evolution of each animal must be extended to a period of couple of days. This suggests a deeper investigation including response to treatment and shock evolution.

5. ACKNOWLEDGEMENTS

We would like to thank Dr. Francisco Soriano and the research group of Laboratory of Medical Investigation of Medical School of University of São Paulo for useful discussions and access to experimental data.

6. REFERENCES

Cerutti, C., Gustin, M.P., Molino, and P. Paultre, C.Z., 2001," Beat-to-beat stroke volume estimation from aortic pressure waveform in conscious rats: comparison of models", Am. J. Physiol. Heart Cir. Physiol, Vol281, pp. H1148-H1155.

Cerutti, C., Gustin, M.P., Paultre, C.Z., Julien, M. Lo, C., Vincent, M., and Sassard, J. 1991, "Autonomic nervous system and cardiovascular variability in rats: a spectral analysis approach", Am. J. Physiol. Heart. Circ. Physiol. Vol. 261, pp. H1292-H1299.

Godje, O., Friedl, R., and Hannekum, A., 2001, "Accuracy of beat-to-beat cardiac output monitoring by pulse contour analysis in hemodynamical unstable patientes", Diagnostics and Med. Tech., Med. Sci. Monit., 7(6), pp. 1344-1350.

Gottschall, C.A.M, 1999, "A maior descoberta do milênio", Arq. Bras. Cardiol., Vol 73, nº 3, pp. 309-319.

Guyton, A.C., 2002, "Tratado de Fisiologia Médica", Editora Guanabara Koogan S/A, Rio de Janeiro, pp. 1014.

Introcaso, L., 1998, "Aspectos Históricos da Hipertensão. História da Medida da Pressão Arterial", Hiperativo,Vol.5, nº2, pp. 79-82.

Mallat, S., 2001, "Wavelet tour of signal processing", 2nd Ed. Elsevier, Academic Press, 620 p.

Parati, G., Mancia, G. Rienzo, M.D., and Castiglioni, P. , 2006, "Point:Counterpoint: Cardiovascular variability is/is not an index of autonomic control of circulation", J. Appl. Physiol, . Vol 101, pp. 676-682.

Rocha, M., Silva, J.R., 1973," Fisiologia da Circulação", Edart, São Paulo.

5. RESPONSIBILITY NOTICE

The authors are the only responsible for the printed material included in this paper.